

# Journal Pre-proof

On the controllability assessment of biofeedback eyeglasses used in Presbyopia treatment

Germán Yamhure, Arturo Fajardo, C.I. Paez-Rueda, Gabriel Perilla, Manuel Pérez



PII: S0141-9382(23)00130-0

DOI: <https://doi.org/10.1016/j.displa.2023.102497>

Reference: DISPLA 102497

To appear in: *Displays*

Received date: 14 April 2023

Revised date: 13 June 2023

Accepted date: 14 July 2023

Please cite this article as: G. Yamhure, A. Fajardo, C.I. Paez-Rueda et al., On the controllability assessment of biofeedback eyeglasses used in Presbyopia treatment, *Displays* (2023), doi: <https://doi.org/10.1016/j.displa.2023.102497>.

This is a PDF file of an article that has undergone enhancements after acceptance, such as the addition of a cover page and metadata, and formatting for readability, but it is not yet the definitive version of record. This version will undergo additional copyediting, typesetting and review before it is published in its final form, but we are providing this version to give early visibility of the article. Please note that, during the production process, errors may be discovered which could affect the content, and all legal disclaimers that apply to the journal pertain.

© 2023 Published by Elsevier B.V.



## On the Controllability Assessment of Biofeedback Eyeglasses Used in Presbyopia Treatment

Germán Yamhure<sup>a</sup>, Arturo Fajardo<sup>a,\*</sup>, C.I. Paez-Rueda<sup>a</sup>, Gabriel Perilla<sup>a</sup>, Manuel Pérez<sup>a</sup>

<sup>a</sup>Department of Electronic Engineering, Pontificia Universidad Javeriana, Calle 40 No. 5-50. Ed. José Gabriel Maldonado S.J., 4to piso, Bogotá D.C. 110311, Colombia

---

### ARTICLE INFO

---

Communicated by Editor

---

**Keywords:**

Biofeedback based on Autofocusing eyeglasses  
 Human control of electrically tunable lenses  
 Presbyopia correction based on Biofeedback

---

### ABSTRACT

---

In recent years, hybrid biofeedback systems utilizing user-controlled electrically tunable lenses have emerged as potential treatments for presbyopia. However, the controllability of these systems, closely linked to user adaptability, has received limited attention in the literature due to the challenges associated with obtaining a comprehensive system model. In this study, we present the design, implementation, and validation of an innovative experimental setup aimed at researching and evaluating the controllability of such a biofeedback system. Our setup incorporates a novel low-complexity model, considering the brain, natural lenses (e.g., the crystalline lens), and electrically tunable lenses, to establish a fundamental model for hybrid biofeedback systems. This model is developed based on an analysis of biofeedback systems, geometrical optics, and control theory, facilitating the identification of strategies to decouple system dynamics and enable precise controllability analysis. The proposed experimental setup was validated with volunteers, providing evidence that confirms the reliable operation of the biofeedback system. Our approach encourages a shift from conventional qualitative approaches toward quantitative evaluation of biofeedback devices. The proposed model and experimental setup hold the potential to statistically assess the controllability of hybrid biofeedback systems for correcting presbyopia, paving the way for further advancements in this field.

---

### 1. Introduction

Presbyopia, a prevalent clinical condition, affects an estimated 1.8 billion individuals worldwide, manifests as a loss in the eye's ability to adjust its refractive or optical power, typically within a few diopters [1, 2, 3]. Presbyopia can be partially corrected through the utilization of a diverse range of optical devices and methodologies [4]. These include multifocal corrective eyeglasses, monovision, and multifocal contact lenses,

as well as smart autofocusing wearable eyeglasses[4, 5, 6, 7, 8, 9, 10].

In conventional approaches utilizing lenses with fixed optical power, the patient's dynamic range is expanded, thereby enabling them to focus at various distances through the resulting biofeedback system [1]. For instance, bifocal eyeglasses incorporate lenses with two distinct optical powers, and the patient can select the desired focal region by adjusting the angle of the craniocervical area and tilting their eyes [11], as illustrated in Fig. 1a. In this biofeedback system, the person actively engages their muscles by alternately relaxing and contracting them to elicit the desired effect [12]. However, certain individuals face

\*Corresponding author:  
 e-mail: [fajardoa@javeriana.edu.co](mailto:fajardoa@javeriana.edu.co) (Arturo Fajardo)

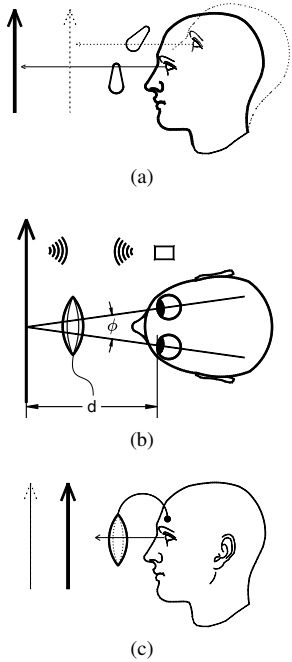


Fig. 1: Presbyopia correction paradigms with eyeglasses. a) Systems based on biofeedback and fixed optical power devices. b) Systems based on distance measurement and electrically tunable lenses. c) Systems based on biofeedback and controlled optical power devices.

challenges in utilizing these methods due to inherent limitations of the eyes, such as disparity vergence [13], or encounter difficulties in adapting to these approaches [14].

Smart autofocusable wearable eyeglasses, utilizing large aperture variable-focus lenses [15], have emerged as a promising solution for correcting presbyopia [4, 5, 6, 7, 8, 9]. The conventional approach for achieving automatic lens accommodation in smart eyeglasses is to calculate the required optical power based on the distance ( $d$ ) between the eyeglasses and the object to be focused, as shown in Fig. 1b. This distance can be measured directly using time-of-flight sensors [4, 6, 7] or indirectly by tracking the person's eye movements [8, 5, 9], both of these measurement techniques are shown in Fig. 1b. The first method requires that the object reflects a strong signal to be detected by the sensor's transducer. Consequently, if the person intends to view objects with low reflectivity (e.g., thin cloth or smoke), this approach limits the ability to achieve correct focus on the object. To overcome this limitation, the second approach utilizes vergence to calculate the distance between the eyeglasses and the object. In this method, a sensor such as a camera is employed to determine the convergence angle ( $\phi$  in Fig. 1b). These systems require an initial calibration procedure in which the person directs their attention to an object at a predetermined distance. Following this calibration phase, the system regulates the optical power of the external lens based on the measured distance between the object and the eyeglasses, assuming a constant optical power of the internal lens. Consequently, the prolonged utilization of such eyeglasses may result in fatigue of the ciliary muscles, as their activity remains nearly constant over an extended duration. This phenomenon closely resembles

computer vision syndrome, characterized by ocular strain and discomfort [16]. It is noteworthy that although directly measuring this phenomenon can be challenging, there are various estimation methods available for assessment [17, 18]. Moreover, in accordance with the Helmholtz-Hess-Gullstrand and Donders-Duane-Fincham theories of presbyopia, the fatigue and discomfort experienced during the extended usage of these eyeglasses could be intensified in individuals with presbyopia.

The Helmholtz-Hess-Gullstrand theory attributes the loss of accommodation in presbyopia solely to the morphological changes in the crystalline lens capsule [19]. Conversely, the Donders-Duane-Fincham theory assigns the age-related decline in accommodation exclusively to the biomechanical properties of the ciliary muscles [19]. According to both theories, as individuals experience a reduction in accommodation, greater effort from the ciliary muscles is required to achieve the same change in optical power. To illustrate this, let's explore the examples discussed below. Based on the Helmholtz-Hess-Gullstrand theory, assuming a dynamic range of 15 diopters (D) during childhood with a linear relationship to the mechanical strength of the muscles, maximum muscle contraction would be needed at 15D. However, as the dynamic range diminishes to only 1D with age, the ciliary muscles must exert the same level of effort as during childhood to accommodate the lens from 14D to 15D, resulting in maximum muscle contraction. In the case of the Donders-Duane-Fincham theory, if the crystalline lens maintains its dynamic range of 15D, the mechanical strength required exceeds that of childhood due to muscle degradation. In both models, the use of an external lens in smart autofocusable wearable eyeglasses improves overall optical power while reducing strain on the ciliary muscle. However, it is important to note that in these eyeglasses, the optical power of the crystalline lens remains relatively constant. As a result, prolonged exertion of the ciliary muscle could result in eye fatigue, impacting individuals with both normal vision and presbyopia. To alleviate this fatigue, it is recommended to engage in relaxing exercises such as yoga [20] or employ an external lens with variable optical power controlled by the person or an automated system. This enables the adjustment of the optical power to achieve focus and relax the associated eye muscles.

In recent advancements within the field of presbyopia correction, a novel approach has emerged that utilizes Electromyography signals (EMG) to control eyeglasses [10]. This innovative biofeedback system offers promising potential for alleviating eye fatigue, particularly ciliary muscle fatigue, by empowering persons to regulate the optical power of their eyeglasses. By exerting control over the internal lens's optical power and subsequently inducing relaxation in the ciliary muscles, individuals can effectively mitigate the strain experienced. Nevertheless, the validation of this prototype primarily relied on subjective person perception tests, with crucial aspects such as the controllability of the biofeedback system left unexplored by the researchers. The controllability of a biofeedback system is a key factor in determining its acceptance, as demonstrated by studies on biofeedback systems that integrate progressive or bifocal lenses [13, 14]. Currently, the assessment of a biofeedback system's performance is limited to subjective tests that fail to

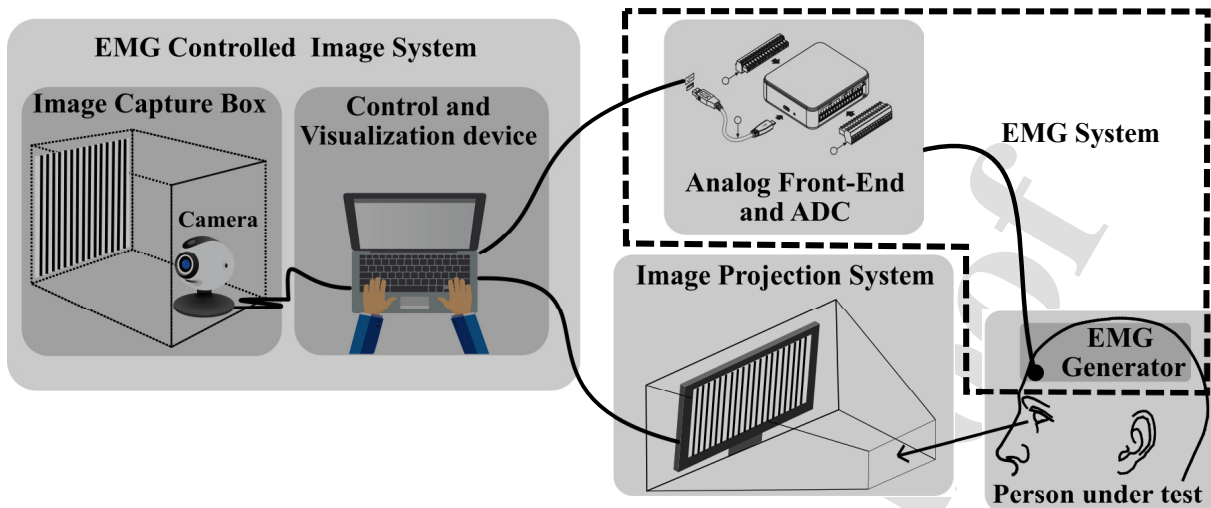


Fig. 2: Block diagram of the proposed system

capture the person's perception of its controllability. The absence of objective information poses significant challenges for biofeedback system designers. Therefore, an important unresolved question in this field relates to the objective measurement of controllability and individual adaptability in such systems.

To the best of the authors' knowledge, no previous study has been conducted on the controllability of this problem. This could be attributed to the lack of a comprehensive model for the biofeedback system, which poses challenges in analyzing its controllability. However, there have been relevant works focusing on modeling the eye's biological system. For example, the modeling of neurological control of accommodation involves a static model that relates the accommodative response to the accommodative stimulus [21]. Furthermore, this modeling approach has recently been employed to enable users to control their autofocusable wearable eyeglasses devices [22]. The procedure involves conducting experiments where patients manually adjust the optical power of tunable lenses in response to changes in the distance to the observed object and lighting conditions.

This article presents an experimental method to investigate and assess the controllability of the biofeedback system described in [10]. We propose a strategy similar to that suggested by [22], with the additional consideration of maintaining constant distance and illumination conditions. This approach aims to reduce the number of variables involved and mitigate their influences, such as variations in pupil aperture. In both approaches, the subject has control over the optical power of external lenses. However, it should be noted that the validation of the model in [22] relies on subjective individual evaluations (such as the Snellen test) rather than objective measurements. The proposed experimental setup, allows for the independent adjustment of each lens within the cascade of lenses, including the camera and the cornea-lens system. This setup, depicted in Fig. 6, comprises the EMG Controlled Image System (CIS), the Image Projection System (IPS), the EMG system, and the Study Participant (SP). The results demonstrate that, following a brief

training period, all volunteers were able to manipulate the camera's focus to enhance image sharpness in the image projection system. The contributions of this paper are as follows:

- Development of a test and experimental setup to evaluate the controllability of biofeedback systems using electrically tunable lenses.
- Designing an experiment to isolate specific physical variables in complex biofeedback systems with electrically tunable lenses.
- Proposing a simplified brain control scheme for optical power devices.
- Introduction a novel taxonomy for the learning, teaching, and evaluation of biofeedback systems.

The paper is structured as follows: Section 2 introduces a simplified optical model of the system proposed in [10] and presents a novel taxonomy of biofeedback systems using a concise theoretical framework. In Section 3, the details of the experimental setup and methods employed in this study are presented. The experimental findings are summarized in Section 4, followed by a discussion on the limitations of this work. Finally, Section 5 presents the conclusions drawn from the study and outlines future research directions.

## 2. Biofeedback system modeling

### 2.1. A brief description of optics in human vision

The person's accommodation capacity refers to their ability to adjust the curvature of their crystalline lenses using the activity of their ciliary muscles, which determines the dynamic range of optical power. This ability allows them to form a clear image of the desired object on the retina. In cases where the accommodation capacity is insufficient, external lenses can provide assistance.

A conventional system utilized for correcting refractive errors of the eye comprises an external lens and the internal eye lenses, along with their associated muscles. Fig. 3 illustrates a simplified optical model of this system, while Fig. 3a presents its schematic representation, and Fig. 3b displays its first-order

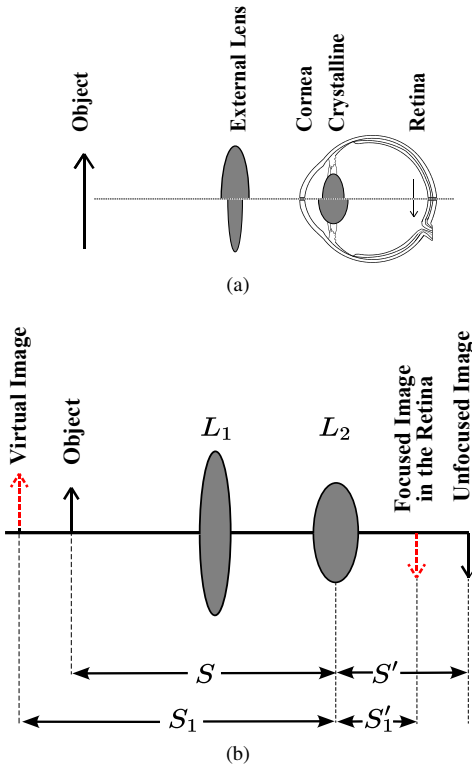


Fig. 3: The simple optical system of human vision. a) Scheme of the system. b) First-order optical model.

**optical model.** Considering that the cornea has a fixed optical power and that only the lens has accommodation capacity, this system is modeled as a single **internal** lens called  $L_2$ . Using this model for positive lenses, the external lens ( $L_1$ ) creates a virtual image at a greater distance from the  $L_2$  reference plane (i.e.,  $S_1 > S$ ). This virtual image is focused by two lenses on the retina, which is located at a distance of  $S'_1$ . If lens  $L_1$  is removed from the correction system, the resulting lens system (i.e., crystalline-cornea) will produce an image  $S'$  from  $L_2$ . As a result, this image is created behind the retina, and the person sees a blurred image of the object. The optical power ( $P$ ) of  $L_1$  required to create an image on the retina is given by [23]:

$$P = \frac{1}{-S_1} - \frac{1}{S}, \quad (1)$$

where  $P$  is given in diopters and  $S_1, S$  are given in meters. Despite its simplicity, this model provides insights into various phenomena associated with human vision. For example, this model allows quantitatively determining (using the maximum optical power of the lens  $L_2$  and  $S'_1$ ) the minimum distance to the object necessary to guarantee a sharp image. Additionally, it also explains why a person with presbyopia should move objects away to improve image sharpness or how the SP can create the image without moving the object by using an external lens. Furthermore, whether an individual has this condition or not, wearing  $L_1$  with user-controlled optical power can potentially reduce the optical power of  $L_2$  by relaxing the ciliary muscle and alleviating eyestrain (asthenopia) associated with prolonged focusing on objects, such as when working in front of

a computer for extended periods. In this context, the user has the ability to adjust the ciliary muscles and modify the optical power of the external lens to suit their needs. The combined optical power of the eye lens and the external lens must match the required power to form a clear image on the retina. This holds true even when considering the aperture adjustment of the pupil, as mentioned in [24].

Whether the object is moving closer or farther away, the described cascade optical system offers two simple solutions to create the image on the retina. The first approach involves keeping the optical power of the external lens constant while adjusting the optical power of the crystalline lens. The second option is to fix the power of the crystalline lens and vary the power of the external lens. However, there are infinite combinations of external lens and crystalline lens powers that can be utilized to form an image on the retina.

In this context, the use of bifocal and progressive lenses is widely employed, enabling individuals to achieve appropriate focus by combining different zones of the external lens with varying optical powers and the optical power of the crystalline lens, as illustrated in Fig. 1a. To enhance image sharpness, individuals can adjust the tilt of their head (craniocervical angle) and the elevation and depression of their eyes. This exemplifies the concept of biofeedback, which involves muscle control, such as the rectus muscles of the eye.

It is important to note that achieving a sharp image on the retina involves a combination of the optical power of the crystalline lens and the opening of the pupil. Furthermore, the model under discussion does not account for the well-known Depth-of-Field (DoF) phenomenon, which defines the range of distances between the lens and the object that result in an image without noticeable blur [21]. The DoF is closely related to depth focus, which quantifies the range of optical power variations in the lens that produce imperceptible changes in blur. While the geometric optics model suggests a single distance known as the hyperfocal distance, the limited resolution of the retina leads to a range of distances, even within the foveal region. Increasing the aperture of the pupil allows more light rays to reach the retina, which can influence the perception of blur. Conversely, pupil constriction expands the DoF, aligning the behavior of the eye's lens system more closely with that of a pinhole camera, which has an infinite DoF.

## 2.2. Brief biofeedback framework

The concept of biofeedback finds wide application in various domains, including rehabilitation, sensory substitution, augmented reality, and sports training [10]. Due to its multidimensionality, the concept of biofeedback has yielded several definitions. On the one hand, the authors in [10] define biofeedback as a process that allows a person to learn to change their physiological activity in order to improve their health and performance. On the other hand, biofeedback is defined in [25] as the process of becoming aware of various physiological functions in order to voluntarily manipulate them at will. This process is developed using instruments that provide information about those functions (e.g., electromyography, skin temperature, heart rate, blood pressure, brain waves, etc.). Finally, in

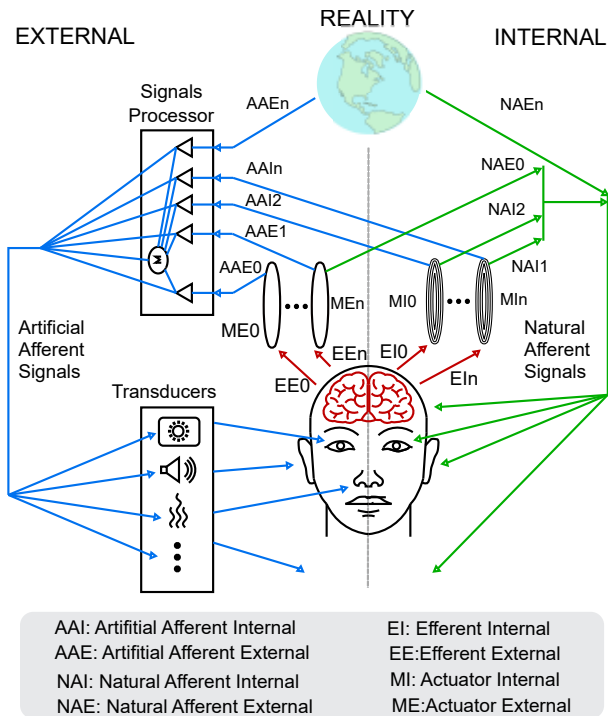


Fig. 4: Block diagram of information flow in biofeedback systems

[26], biofeedback is defined as a control system related to the human body that operates on two elements: a natural and an artificial biofeedback mechanism. Natural biofeedback is described as a mechanism for regulating the human body's functioning. Artificial biofeedback is presented as a control system equipped with sensors that alert the person to interact with some natural regulatory mechanism controlled by the brain.

Inspired by the human nervous system and the aforementioned biofeedback definitions, we propose a comprehensive biofeedback-system information-flow diagram, as depicted in Fig. 4. The diagram elucidates the afferent flow, which represents the information flow from peripheral elements (e.g., organs, muscles, external objects) to the control unit (i.e., the

brain). Conversely, the efferent information flow is defined as the flow from the control unit to the periphery elements. Within this diagram, an efferent action or information flow is represented by arrows labeled as EI (Efferent Internal-nth) or EEn (Efferent External-nth), while afferent actions or information flows are illustrated by arrows labeled as AAIn (Artificial Afferent Internal-nth), AAEn (Artificial Afferent External-nth), NIn (Natural Afferent Internal-nth), and NAEEn (Natural Afferent External-nth).

The proposed biofeedback diagram serves as a valuable tool for understanding the diverse contexts in which biofeedback is applied. For instance, it elucidates the information flow required to perceive the external environment, referred to as "REALITY" in the Fig. 4. This perception is achieved through afferent information flow from the human senses to the brain. Another example involves the process of picking up an object, where the brain controls the action through efferent and afferent actions generated by feedback and learning mechanisms. Specifically, the brain activates the appropriate muscular system to move the hand in a specific direction (efferent action), while muscle spindles provide proprioception information, indicating the hand's position at each moment in time (afferent action). Consequently, the brain successfully accomplishes the task of picking up the object. Moreover, in the context of enhancing the learning process of fine motor skills in highly competitive athletes, muscular activity is captured using a signal processor, such as electromyography (EMG). This captured information is presented to the athlete via a screen (external afferent information flow), allowing them to perceive and interpret the information visually (internal afferent information flow). The athlete utilizes this information to adjust and refine their muscle movements (external afferent action). As a result of such biofeedback-driven training, athletes experience improvements in their performance.

By analyzing the proposed diagram and relevant literature, we proposed a taxonomy that categorizes various types of biofeedback, which is summarized in Table 1. Additionally, the table highlights applications associated with each type of biofeedback.

Table 1: A simple taxonomy of biofeedback types

Biofeedback type	Afferent Flow	Efferent Flow	Application Examples
Natural	Internal	Internal	Natural blood glucose control [26]
Afferent Artificial	External	Internal	1. Rehabilitation of Motor Function [27, 28, 29, 30, 31, 32] 2. Breathing control as a mechanism for controlling muscular stress [33, 34]
Efferent Artificial	Internal	External	Blind people use canes to navigate their surroundings [35]
Fully Artificial	External	External	Virtual reality games [36, 37].
Hybrid	Internal and/or External		1. Internal-afferent and external-internal efferent flow: use of EMG-controlled optical power lenses. [4, 5, 6, 7, 8, 9] 2. Afferent and efferent flow both internal and external: Insulin pump to help with blood glucose control [26].

317 **2.3. Modeling of the brain control involved in biofeedback sys-  
318 tems based on electrically tunable lenses**

319 This study presents a modeling approach to understand the  
320 brain control involved in biofeedback systems utilizing electric-  
321 cally tunable lenses to achieve sharp image projection onto the  
322 retina. The eyeglasses biofeedback systems based on distance  
323 measurement and controlled optical power devices (shown in  
324 Fig. 1b) establish the optical power of the external lens (i.e., L1  
325 in Fig. 3b). As a natural biofeedback system, the user can inter-  
326 vene by adjusting the line of sight and vergence. However, the  
327 external device determines the vergence distance and calculates  
328 the optical power of the external lens, thereby denying the user  
329 any degree of control over the optical power of the crystalline  
330 lens. Consequently, the user must adapt to the external device's  
331 settings. Under this approach, the optical power of the crys-  
332 talline lens (i.e., L2) is almost constant. The proposed system  
333 shows a distance estimation error that the user can correct by  
334 changing the optical power of the lens until the desired sharp-  
335 ness is achieved. As a result, this feedback system is natural  
336 (as defined in Table 1) and it is assumed to be perfectly sta-  
337 ble. In addition, as we discussed in Section 2.1, a variety of  
338 lens optical power combinations (i.e., L1 and L2) could pro-  
339 duce a sharpness image in eyeglasses biofeedback systems that  
340 do not require distance measurement. In these systems, the user  
341 can control the optical power of the external lens (i.e., L1) by  
342 inclining the neck (and eyes) or modifying the myoelectric ac-  
343 tivity of a muscle (e.g., corrugator superciliary muscle [10]), as  
344 shown in the figures 1a and 1c. The user can also adjust the  
345 optical power of the crystalline lens (i.e., L2). As a result, this  
346 biofeedback system is a hybrid one (as defined in Table 1), and  
347 its controllability cannot be guaranteed. Furthermore, there is  
348 some evidence of some people's inability to adapt to the use of  
349 eyeglass biofeedback systems based on bifocal and progressive  
350 lenses (i.e., the system shown in Fig. 1a) [14]. It is crucial to  
351 recognize the importance of a functional model for analyzing  
352 the controllability of the system. This compact model aids in  
353 determining the optical power of the external lenses in the pres-  
354 byopia correction system that utilizes tunable lenses. However,  
355 it should be noted that with the proposed model and its experi-  
356 mental setup, it is not possible to evaluate the system's control-  
357 lability because the brain control involved in the proposed setup  
358 is not considered.

359 In our literature review, we have identified a limited num-  
360 ber of studies that have addressed the modeling aspect of pres-  
361 byopia correction systems using tunable external lenses. One  
362 notable example is the work by [22], where they propose an  
363 experimental setup allowing patients to manually control the  
364 optical power of external lenses. The Snellen test is employed  
365 to assess visual acuity, considering variations in distance and  
366 lighting conditions. Based on the obtained results, the authors  
367 develop individual-specific compact empirical models of sub-  
368 jective accommodative error based on the model proposed in  
369 [38]. This compact model aid in determining the optical power  
370 of the external lenses in the presbyopia correction system util-  
371 izing tunable ones. However, it should be noted that, to the  
372 best of our knowledge, this particular model does not facilitate  
373 the evaluation of the system's controllability. Furthermore, it is  
374 crucial to recognize the importance of a functional model for  
375 analyzing the controllability of the system.

376 To address the modeling gap identified, we propose a sim-  
377 plified model of smart eyeglasses based on tunable lenses. In  
378 this proposed model, the output variable of the human vision  
379 system can be defined as image sharpness, which is influen-  
380 ed by several factors [39, 40]:

- 381 • Multiple actuators, such as the muscles associated with the  
382 optical power control of the involved lens (e.g., crystalline  
383 and external lens), the rectus muscles of the eye, the mus-  
384 cles associated with pupil opening and closing, and the  
385 muscles associated with changes in the axial length of the  
386 eyeball [40], among others, play a role in the biofeedback  
387 system.
- 388 • External factors, such as the speed of object movement,  
389 image contrast, ambient lighting, and other variables de-  
390 tected by the system, can modify its functionality.
- 391 • A powerful control system (i.e., the brain) stands out for its  
392 remarkable plasticity and learning capacity. It controls the  
393 various actuators involved and analyzes data from related  
394 sensors to achieve the desired sharpness. Additionally, the  
395 control actions are directly influenced by the individual's  
396 intention, such as focusing on a specific object in a scene.

397 The simple model, shown in Fig. 5, allows comprehension  
398 of the eyeglasses system proposed in [10]. This model only  
399 takes into account two sharpness control loops and the main

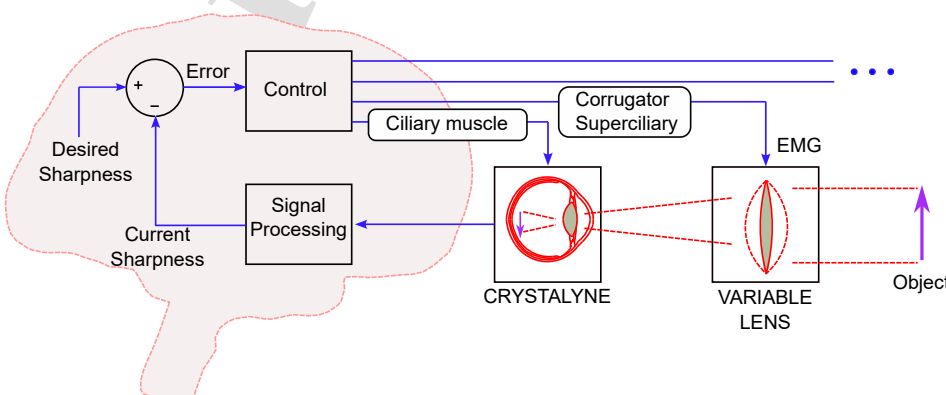


Fig. 5: Simplified brain control model for electrically tunable lenses

400 system actuators (Ciliary muscle and Corrugator Superciliary).  
 401 Despite the significant simplifications, the model reflects the  
 402 operational complexity of the control brain as well as the fact  
 403 that the system has an infinite number of solutions.

#### 404 2.4. On the objective assessment of electrically tunable eye- 405 glasses' controllability

406 The Snellen test is used to determine the required optical  
 407 power in the traditional approach to improving human vision  
 408 with eyeglasses. This test involves an examiner changing the  
 409 external lenses and receiving feedback from a patient on the  
 410 sharpness perception of projected letters and symbols of vary-  
 411 ing sizes. Therefore, the obtained result may contain significant  
 412 biases due to subjective assessment of sharpness, for which the  
 413 examiner confirms the person's ability to identify the symbols.  
 414 This check helps to reduce the bias introduced by the patient.  
 415 However, to avoid test subjectivity, the user's assessment must  
 416 be removed.

417 Given the enormous difficulty of obtaining a system model  
 418 and the desire to analyze the controllability of the biofeedback  
 419 system proposed in [10], one possible approach is to implement  
 420 a platform that decouples the control of the external lens from  
 421 the other actuators involved in image focusing (primarily the  
 422 crystalline lens) under controlled conditions. The design goals  
 423 of this type of platform are as follows:

- 424 • Maintain a constant distance between the user and the ob-  
 425 served object.
- 426 • Control the lighting environment to keep the pupil opening  
 427 almost constant.
- 428 • Keep the eyes in the same relative position to the object to  
 429 avoid vergence.
- 430 • Limit saccadic movements by avoiding the presence of  
 431 points of greater attention using a spatially and static pro-  
 432 jected image.
- 433 • Limit peripheral vision to avoid user distractions.
- 434 • Minimize the impact of varying pupil apertures by main-  
 435 taining almost constant lighting conditions.

436 To meet this challenge, we propose the platform depicted in  
 437 figures 2 and 6. This experimental setup will be explained in  
 438 detail in Subsection 3.2.

### 439 3. Proposed biofeedback system

#### 440 3.1. A brief restrictions context

441 As explained in [21], the sensory and motor pathways re-  
 442 sponsible for blur-driven accommodation constitute a complex  
 443 process. This process involves the contraction of the ciliary  
 444 muscles, which modifies the shape of the crystalline lens based  
 445 on the image projected onto the retina. Accommodation encom-  
 446 passes several components, including reflex, vergence, prox-  
 447 imal, and tonics, which incorporate subjective perception, ex-  
 448 periential appraisals, and other brain processes. Consequently,  
 449 the control of external lenses based on neurological signals re-  
 450 mains an ongoing challenge due to the inherent complexity in-  
 451 volved. To mitigate the need for brain-computer interfaces, the  
 452 direct brain control has been replaced in some smart eyeglasses

453 implementations by alternative methods such as measuring the  
 454 distance between the user and an object or utilizing the EMG  
 455 signal from a facial muscle to regulate the optical power of the  
 456 external lenses [4, 5, 6, 7, 8, 9, 10].

457 In [10], the authors utilize a signal processing strategy to  
 458 monitor the activity of the superciliary corrugator muscle for  
 459 regulating the power of external lenses, rather than relying on  
 460 direct brain control. This approach is commonly employed in  
 461 biofeedback systems. A classic example of this concept is the  
 462 control of a computer mouse, where the user's brain serves as  
 463 a direct controller of hand muscles, indirectly affecting the  
 464 cursor's position on the screen. The superciliary corrugator muscle  
 465 (along with neighboring muscles) is frequently engaged during  
 466 visual tasks and it is known to contribute to the improvement  
 467 of visual perception. Furthermore, this contribution is the same  
 468 effect as a pinhole camera, improving the depth of focus and  
 469 subtly altering lens curvature [21].

470 The proposed experimental setup allows for the evaluation  
 471 of the controllability of systems based on superciliary muscle  
 472 EMG control, such as the one proposed in [10], under con-  
 473 trolled conditions. This approach minimizes the number of en-  
 474 vironmental and physiological variables, as well as their inter-  
 475 actions. To ensure consistency, the study imposed restrictions  
 476 on the age, physical condition, and visual health of the partici-  
 477 pants. The test group comprised five young university students,  
 478 ranging in age from 23 to 26 years, who did not have any optical  
 479 or physical diseases.

#### 480 3.2. Experimental setup description

481 An experimental setup was implemented to quantitatively an-  
 482alyze the capability of the SP to control an external optical  
 483 power device. This setup is depicted in Fig. 6. In the pro-

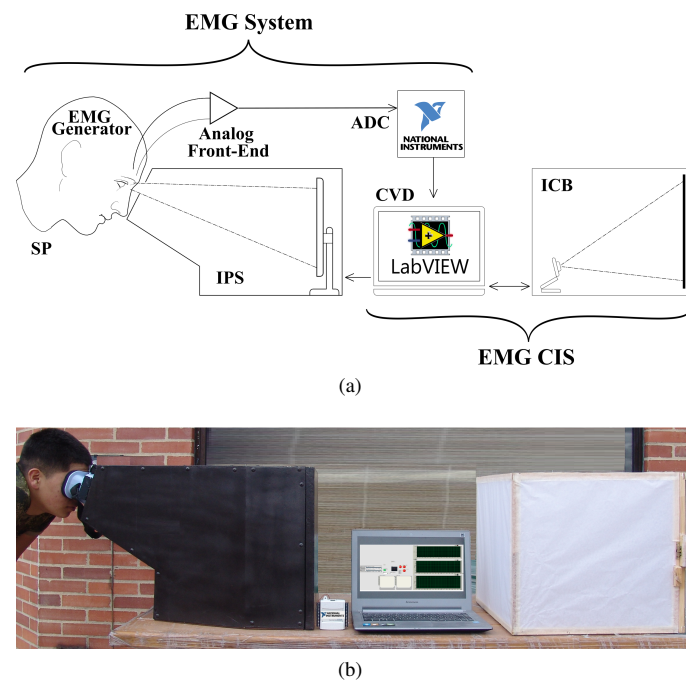


Fig. 6: Experimental Setup. (a) Diagram.(b) Photograph.

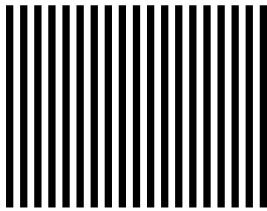


Fig. 7: Selected pattern using in the experimental setup.

posed platform, a black-and-white pattern image (Fig. 7) is positioned at a fixed distance from a camera with controllable focus, specifically the Logitech C920 Full HD. The setup is conducted under semi-controlled lighting conditions, with diffuse lighting at approximately 300 lux, adhering to the illuminance level recommended by the IESNA for meeting rooms [41]. The camera's image is then transmitted to a computer, which displays it on a screen. This visual display unit is placed within a matte black box, both on the outside and inside, featuring a visual aperture. The SP observes the image on the screen through the aperture at a constant distance of 55 cm, intentionally chosen to minimize vergence changes. Eye blinkers are used during observation, and the distance is set greater than the SP's minimum focusing distance. The SP may wear corrective glasses if necessary.

The projected image in the IPS may initially be out of focus, prompting the SP to attempt to focus the image by engaging their corrugator muscles, which generates an EMG signal. This signal is detected by the EMG system using an active electrode (specifically, the Z03-003 manufactured by Motions Lab Systems) placed on the muscle. The EMG signal is then processed and transmitted to the EMG CIS system, which controls the focus of the camera located in the image capture box. The captured image pattern is subsequently sent back to the IPS system to close the biofeedback loop. As a result, if the screen image is sharp (indicating successful camera focusing) and the user determines the required optical power of the crystalline lens to focus the screen, the SP perceives a sharp image. This platform effectively decouples camera control from the rest of the optical system, enabling an objective assessment of its controllability.

The EMG signal is captured by the EMG Generator (i.e., electrodes and the SP) and is processed through several stages in the analog front-end and Analog-to-Digital Converter (ADC) system. These stages involve an active electrode, instrumentation amplifier, filter, and isolated amplifier with digital programmable gain. For reducing common noise produced by the 60 Hz power line, we selected the active electrode Z03-003, which provides a voltage gain of 300 V/V and a common mode rejection ratio (CMRR) greater than 100 dB within a Signal Bandwidth of 15 Hz to 2 kHz [42]. The next amplifier stage utilizes an INA128 instrumentation amplifier [43] with a user-selectable gain and a CMRR exceeding 130 dB, effectively maintaining low 60 Hz noise.

The active multistage filter, implemented with OPA2132 operational amplifier [44], is a third-order band-pass filter with a low cutoff frequency of 25 Hz and a high cutoff frequency of 500 Hz. This frequency range aligns with the guidelines of the

European organization SENIAM (Surface ElectroMyoGraphy for the Non-Invasive Assessment of Muscles), which recommend low-cut frequencies around 20 Hz and high-cut frequencies up to 1 kHz to mitigate artifacts caused by muscle-skin and electrode-skin motion [45]. References [46] and [47] support the selection of this frequency range, with [46] suggesting a low-cut frequency of 15-28 Hz for facial muscles and [47] analyzing the spectral density function of the EMG and identifying the relevant frequency range as 8 Hz to 500 Hz.

The active filter also serves as an antialiasing filter for the ADC, which is integrated into the Multifunction I/O Device USB6366 [48] and operates at a sampling frequency of 10 kS/s and 16 bits, as recommended by SENIAM [45]. The isolated amplifier with digitally programmable gain consists of two stages, with the isolated stage utilizing AMC 1200 [49] and the programmable gain stage employing PGA 281 [50].

After the processing of the EMG signal in the analog front-end and Analog-to-Digital Converter (ADC) system, the digital EMG signal is transmitted to the EMG CIS system. The control and visualization device (CVD) encompasses several steps. Firstly, a software-adjustable digital notch filter is employed to further mitigate power line noise. Secondly, to prevent system saturation, the gain of the programmable amplifier is adjusted using the software interface and set below the Maximum Voluntary Contraction (MVC) of the SP. Thirdly, the CVD calculates the Root Mean Square (RMS) of the received digital EMG signal. Fourthly, the CVD establishes a communication link with the camera responsible for capturing the pattern image in the Image Capture Box (ICB). This link serves two purposes: receiving the captured image and adjusting the camera focus based on the RMS value of the digital EMG signal.

Finally, the CVD transmits the image to the IPS system, which comprises an image projection box, a digital screen, eye blinkers, and the SP. The image projection box isolates the screen projection from external lighting conditions, while the blinkers restrict the SP's peripheral vision. Additionally, the overall process is visualized and stored in a user interface. These functionalities are implemented on a dedicated computer using LabView software.

### 3.3. Experimental test protocol

To quantitatively validate the control capacity of the SP an experiment was designed to resolve the following question: The SP could control the camera's optical power to focus the projected image. The proposed experiment uses the experimental setup described in Section 3.1 and the protocol detail below:

1. After instructing the SPs to perform the MVC and to minimize EMG signal distortion, it is necessary to adjust the voltage gain of the system to prevent voltage saturation of the amplifiers involved.
2. Locate the 43x28 cm printed pattern (see Fig. 7) at a distance of 25 cm from a camera with a resolution of 430x240 pixels which captures images at 30 frames per second into the image capture box under semi-controlled lighting conditions.
3. Run an auto-focus program and store the Focus Indicator (FI) value, which is a number from 0 to 256 generated by the camera.

- 588 4. Install an active electrode pair on the forehead to read the  
589 SP EMG activity.  
590 5. Locate the SP in the IP system facing semi-controlled  
591 lighting conditions and restricted vision.  
592 6. Begin a training period. This stage of the experiment will  
593 last for as long as the volunteer feels comfortable with the  
594 overall system, which is limited to one hour.  
595 7. Start the experiment. After a few seconds of observing the  
596 focused image, the program abruptly blurs the image on  
597 the screen (changes the FI).  
598 8. Sense and store the EMG activity of the SP due to his/her  
599 muscular activity.  
600 9. Modify and store the FI based on the sensed EMG activity.  
601 10. Finish the experiment when the FI is set to a value that is  
602 equal to or less than the value discovered during the auto-  
603 focus procedure.

The experiment was conducted eight times following the adaptation phase, once the test subjects felt comfortable using the camera's control. The final test was excluded to mitigate the potential bias introduced by fatigue. Additionally, the first two tests were excluded from the dataset as they were deemed part of the training phase. Consequently, the analysis focuses exclusively on the normalized results derived from the remaining five tests.

### 612 3.4. Experimental waveform description

613 The typical waveforms of the FI and RMS EMG signals in  
614 the experiment are shown in Fig. 8. At time zero, the program  
615 rapidly defocuses the image, initiating a delay phase that  
616 continues until the SP begins controlling the focus using the RMS  
617 EMG signal. This is followed by the set focus phase, where the  
618 SP increases its EMG activity to enhance image sharpness. If

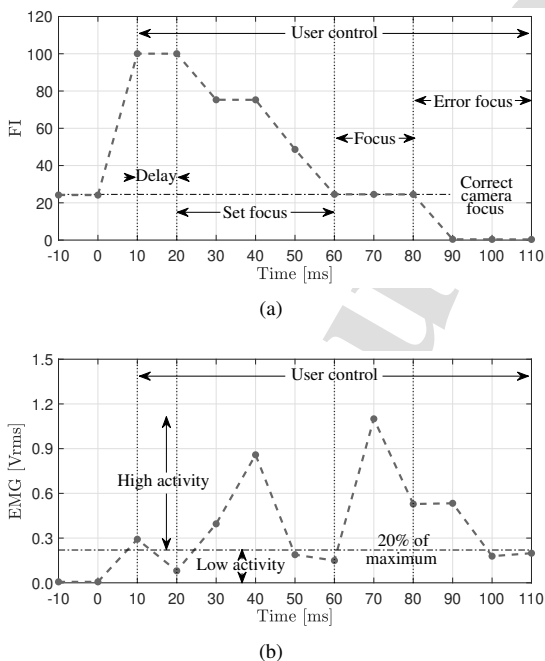


Fig. 8: Typical experimental waveforms. (a) Camera Focus Indicator (FI) vs time. (b) Electromyography (EMG) vs time.

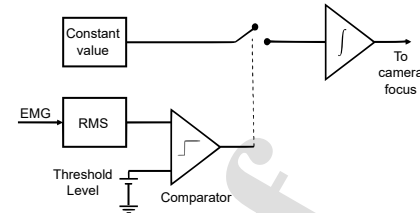


Fig. 9: Control algorithm of the camera focus.

the SP's EMG activity remains below a certain threshold, the image focus remains constant. The control logic for this process is illustrated in Fig. 9. In this algorithm, the camera focus increases steadily as the EMG activity of the superciliary corrugator muscle exceeds a threshold value, which is set as the 20% MVC RMS value. Setting thresholds below 2.5% MVC RMS presents challenges in detecting changes in the power spectral density function, while excessively high values can lead to subject fatigue [47]. Upon reaching the end of the set focus phase, the SP achieves the sharpest image. Subsequently, the SP maintains low EMG activity briefly in the focus phase before attempting to improve sharpness again in the error focus phase. However, these attempts are unsuccessful because the system can only correct image focus by increasing the optical power of the tunable lenses, not decreasing it. It is worth noting that the proposed control strategy incorporates an integral action, resulting in a time delay between the FI and EMG waveforms.

## 4. System results

The experimental waveforms of the FI and RMS EMG signals are presented in Fig. 10. Additionally, Figures 11 and 12

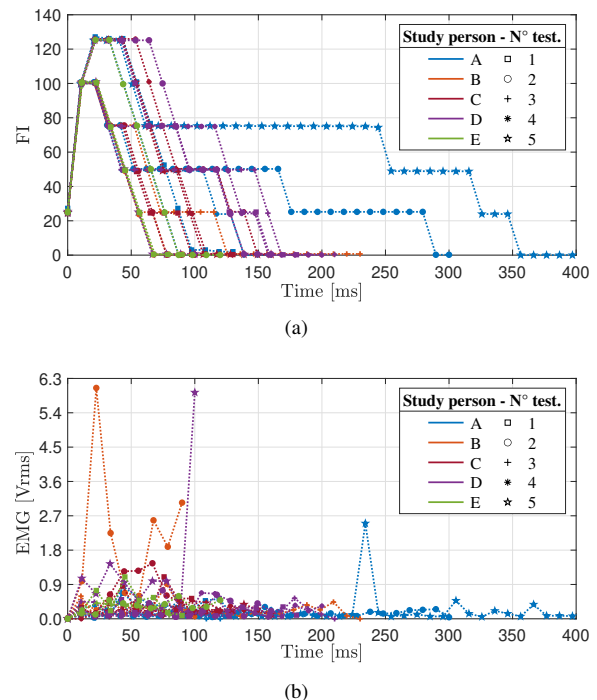


Fig. 10: Experimental waveforms. (a) FI vs time.(b) EMG vs time.

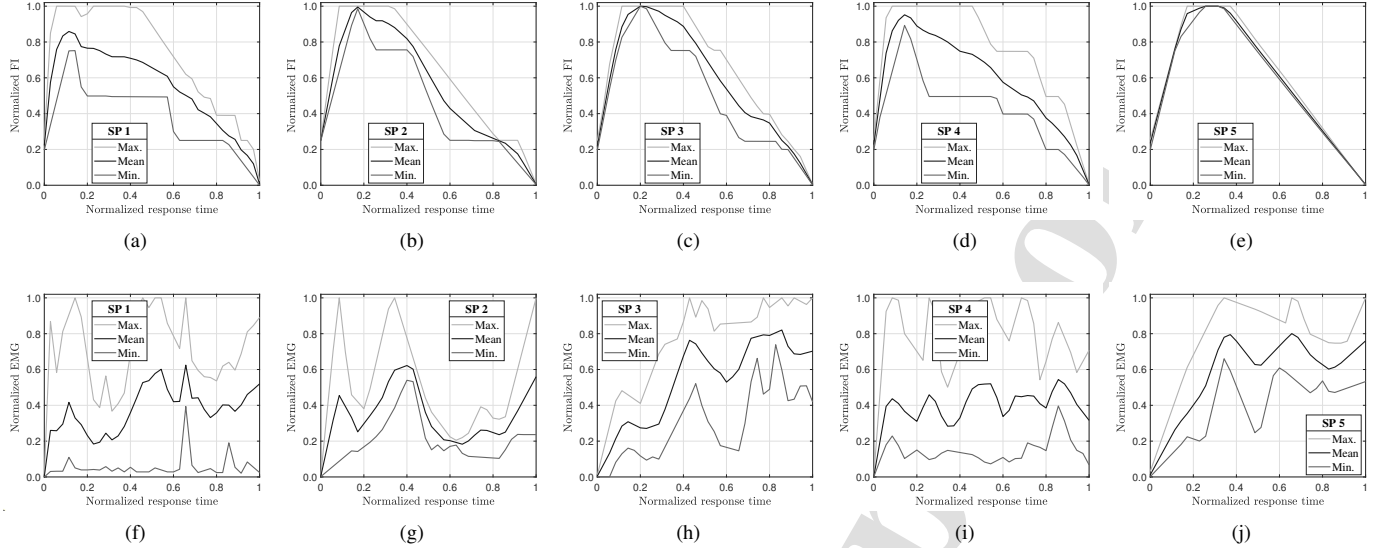


Fig. 11: Experimental Normalized waveforms by person. (a) FI SP 1. (b) FI SP 2. (c) FI SP 3. (d) FI SP 4. (e) FI SP 5. (f) EMG SP 1. (g) EMG SP 2. (h) EMG SP 3. (i) EMG SP 4. (j) EMG SP 5.

639 summarize the resulting statistics, including the mean, maximum,  
 640 maximum, and minimum values of the normalized waveforms, to  
 641 analyze the main behaviors of the SPs at both individual and  
 642 overall participant levels. It is worth noting that the camera's  
 643 focusing time (less than 50 ms) surpasses the human accommodation time (ranging from 400 ms to 1000 ms [7]), which is  
 644 crucial for interpreting these findings.  
 645

646 The waveform shown in Fig. 10a illustrates the consistent  
 647 improvement in camera focus achieved by the SPs after the  
 648 training stage. Notably, this improvement is accompanied by  
 649 significant inter-person variation, which is commonly observed  
 650 in experiments involving human participants. Furthermore, the  
 651 typical response time for switching from an unfocused to a fo-  
 652 cused image ranges from 50 to 350 milliseconds. This response  
 653 time aligns with the reported literature on the time required to  
 654 transition between far and near vision (i.e., 350 ms [7]).

655 Based on the analysis presented in Fig. 11, it can be ob-  
 656 served that SP 1 and SP 4 exhibit a considerable dispersion of  
 657 data points in comparison to their respective means. This higher  
 658 dispersion could potentially be attributed to training lag. Fur-  
 659 thermore, when considering the mean values of each SP, it is  
 660 evident that the RMS EMG and the associated focus strategy  
 661 vary among individuals. For instance, SP 1, SP 2, and SP 4  
 662 are characterized by an initial high effort, followed by a brief  
 663 decrease, and eventually, a final high effort to complete the ex-  
 664 periment. However, regardless of these individual variations, all  
 665 SPs demonstrate the ability to reduce the FI through their con-  
 666 trol actions, thereby enabling the adjustment of camera focus  
 667 and enhancing the sharpness of the projected image. This ad-  
 668 justment continues until the final FI matches the value obtained  
 669 through the camera's autofocus function.

670 Considering the mean values of the overall SPs in Fig. 12,  
 671 the person can reduce the FI with their EMG activity using the  
 672 proposed biofeedback setup. Furthermore, in the control user  
 673 stage, this activity is characterized by a higher increase at the

674 start of the stage and a constant activity until the end of the  
 675 test, even after image focus is reached because the SP can only  
 676 change the focus in one direction.

## 5. Conclusions

677 An experimental method for studying and evaluating the  
 678 controllability of eyeglasses based on biofeedback and tunable  
 679 lenses was implemented and assessed in this article. Although  
 680

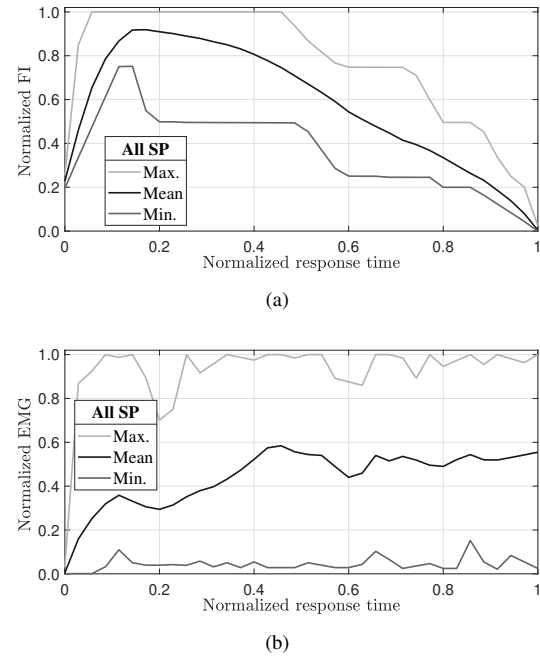


Fig. 12: Overall experimental waveforms. (a) Camera Focus Indicator vs time.  
 (b) Electromyography vs time.

each volunteer uses a different focusing technique after the training phase, all users were able to control the systems and achieve the setpoint (i.e., a sharp image on the screen). The response time from an unfocused to a focused image was between 50 and 350 milliseconds, which is consistent with the human natural focus times. The proposed experimental setup, as demonstrated in the paper, was very useful for objectively assessing the controllability of systems based on eyeglasses with power controller lenses.

In our future work, we plan to enhance the proposed platform by implementing the following improvements: 1) Adding the capability to adjust the camera's focus in both directions to replicate human vision more accurately. 2) Utilizing a camera to measure the pupil diameter while observing the SP. This measurement will help us to evaluate whether the pupil diameter remains constant due to consistent illumination or if it changes as a result of variations in the contrast of the projected image. 3) Future research endeavors are planned to involve older individuals with presbyopia and/or other visual diseases. This expansion of the participant pool will allow for the investigation of the effects of visual diseases on the controllability of smart eyeglasses based on superciliary muscle EMG control.

## Acknowledgments

The authors would like to thank the Laboratory of the Electronics Engineering Department for the support and the Pontificia Universidad Javeriana for the funding for the publication of this paper.

## References

- [1] M. Katz, P. Kruger, Chapter 33: The human eye as an optical system, Duane's Clinical Ophthalmology. Philadelphia, PA: Lippincott, Williams & Wilkins (2013).
- [2] J.D. Silver, D.N. Crosby, G.E. MacKenzie, M.D. Plimmer, ????, URL: <http://www.icoptix.com/wp-content/uploads/2014/07/Centre-for-Vision-in-Dev-world-Oxford.pdf>.
- [3] T.R. Fricke, N. Tahhan, S. Resnikoff, E. Papas, A. Burnett, S.M. Ho, T. Naduvilath, K.S. Naidoo, Global prevalence of presbyopia and vision impairment from uncorrected presbyopia: systematic review, meta-analysis, and modelling, *Ophthalmology* 125 (2018) 1492–1499.
- [4] M.U. Karkhanis, C. Ghosh, A. Banerjee, N. Hasan, R. Likhite, T. Ghosh, H. Kim, C.H. Mastrangelo, Correcting presbyopia with autofocus liquid-lens eyeglasses, *IEEE Transactions on Biomedical Engineering* 69 (2021) 390–400.
- [5] N. Padmanaban, R. Konrad, G. Wetzstein, Autofocals: Evaluating gaze-contingent eyeglasses for presbyopes, *Science advances* 5 (2019) eaav6187.
- [6] N. Hasan, M. Karkhanis, F. Khan, T. Ghosh, H. Kim, C.H. Mastrangelo, Adaptive optics for autofocus eyeglasses, in: *Imaging and Applied Optics 2017 (3D, AIO, COSI, IS, MATH, pcaOP)*, Optica Publishing Group, 2017, p. AM3A.1. URL: <http://opg.optica.org/abstract.cfm?URI=AIO-2017-AM3A.1>. doi:10.1364/AIO.2017.AM3A.1.
- [7] J. Jarosz, N. Molliex, G. Chenon, B. Berge, Adaptive eyeglasses for presbyopia correction: an original variable-focus technology, *Optics express* 27 (2019) 10533–10552.
- [8] J. Mompeán, J.L. Aragón, P. Artal, Portable device for presbyopia correction with optoelectronic lenses driven by pupil response, *Scientific Reports* 10 (2020) 1–9.
- [9] T. Fujita, S. Sato, M. Idesawa, A gazing point distance detection system for accommodation assisting glasses, in: *SENSORS, 2002 IEEE*, volume 2, IEEE, 2002, pp. 905–910.
- [10] R. Linero-Ramos, G. Yamhure-Kattah, J. Gomez-Rojas, Evaluation of the improvement in visual acuity using electronic system biofeedback, *Journal of Xi'an University of Architecture & Technology* 12 (2020) 1401–1411.
- [11] T. Inoue, Vdt eyeglasses—multifocal lenses for near distance use, *Displays* 23 (2002) 11–16.
- [12] G.A. da Silva, P.A. Nogueira, R. Rodrigues, Multimodal vs. unimodal biofeedback in videogames: an empirical player study using a first-person shooter, in: *2014 9th Iberian Conference on Information Systems and Technologies (CISTI)*, IEEE, 2014, pp. 1–6.
- [13] C.A. Castillo, B. Gayed, C. Pedrono, K.J. Ciuffreda, J.L. Semmlow, T.L. Alvarez, The transient component of disparity vergence maybe an indication of progressive lens acceptability, in: *2006 International Conference of the IEEE Engineering in Medicine and Biology Society*, IEEE, 2006, pp. 5687–5690.
- [14] T.L. Alvarez, S. Han, C. Kania, E. Kim, O. Tsang, J.L. Semmlow, B. Granger-Donetti, C. Pedrono, Adaptation to progressive lenses by presbyopes, in: *2009 4th International IEEE/EMBS Conference on Neural Engineering*, IEEE, 2009, pp. 143–146.
- [15] J.F. Algorri, D.C. Zografopoulos, V. Urruchi, J.M. Sánchez-Pena, Recent advances in adaptive liquid crystal lenses, *Crystals* 9 (2019) 272.
- [16] M. Rosenfield, Computer vision syndrome: a review of ocular causes and potential treatments, *Ophthalmic and Physiological Optics* 31 (2011) 502–515.
- [17] A. Kuwahara, K. Nishikawa, R. Hirakawa, H. Kawano, Y. Nakatoh, Eye fatigue estimation using blink detection based on eye aspect ratio mapping(earm), *Cognitive Robotics* 2 (2022) 50–59.
- [18] H. Richter, T. Bänziger, S. Abdi, M. Forsman, Stabilization of gaze: A relationship between ciliary muscle contraction and trapezius muscle activity, *Vision Research* 50 (2010) 2559–2569. *Vision Research Reviews*.
- [19] W.N. Charman, The eye in focus: accommodation and presbyopia, *Clin Exp Optom* 91 (2008) 207–225.
- [20] S.K. Gupta, S. Aparna, Effect of Yoga Ocular Exercises on Eye Fatigue, *Int J Yoga* 13 (2020) 76–79.
- [21] K.J. Ciuffreda, Accommodation, the pupil, and presbyopia, *Borish's clinical refraction* (2006) 93–144.
- [22] M.U. Karkhanis, A. Banerjee, C. Ghosh, R. Likhite, E. Pourshaban, H. Kim, D.A. Meyer, C.H. Mastrangelo, Compact models of presbyopia accommodative errors for wearable adaptive-optics vision correction devices, *IEEE Access* 10 (2022) 68857–68867.
- [23] K.B. Wolf, Geometric optics on phase space, Springer Science & Business Media, 2004.
- [24] A. Prado Montes, Á. Morales Caballero, J.N. Molle Cassia, Síndrome de fatiga ocular y su relación con el medio laboral, *Medicina y seguridad del trabajo* 63 (2017) 345–361.
- [25] T. Wang, The review of biofeedback and its mechanism, *Medical Information* 15 (2002) 610–614.
- [26] R. Li, D.T. Lai, W. Lee, A survey on biofeedback and actuation in wireless body area networks (wbans), *IEEE reviews in biomedical engineering* 10 (2017) 162–173.
- [27] M. Semprini, A.V. Cuppone, I. Delis, V. Squeri, S. Panzeri, J. Konczak, Biofeedback signals for robotic rehabilitation: Assessment of wrist muscle activation patterns in healthy humans, *IEEE Transactions on Neural Systems and Rehabilitation Engineering* 25 (2017) 883–892.
- [28] L. Carvalho, H. Albuquerque, C. Pontes, M. Maia, D. Mangueira, L. Batista, Computerized biofeedback tool: application in electromyogram-biofeedback, in: *Proceedings of the 25th Annual International Conference of the IEEE Engineering in Medicine and Biology Society (IEEE Cat. No.03CH37439)*, volume 2, 2003, pp. 1609–1612 Vol.2. doi:10.1109/IEMBS.2003.1279674.
- [29] D. Shuhan, H. Tanabe, Y. Morita, Z. Peichen, Effect of introducing emg biofeedback to a finger extensor facilitation training device for hemiplegic patients after strokes, in: *2019 19th International Conference on Control, Automation and Systems (ICCAS)*, 2019, pp. 184–187. doi:10.23919/ICCAS47443.2019.8971742.
- [30] Y. Fang, Z.F. Lerner, Feasibility of augmenting ankle exoskeleton walking performance with step length biofeedback in individuals with cerebral palsy, *IEEE Transactions on Neural Systems and Rehabilitation Engineering* 29 (2021) 442–449.
- [31] J. Ling, J.C. Hong, Y. Hayashi, K. Yasuda, Y. Kitaji, H. Harashima, H. Iwata, A haptic-based perception-empathy biofeedback system with vibration transition: Verifying the attention amount, in: *2020 42nd IEEE International Conference on Systems, Man, and Cybernetics (SMC)*, 2020, pp. 1–6. doi:10.1109/SMC50534.2020.9207003.

- 813 Annual International Conference of the IEEE Engineering in Medicine  
 814 and Biology Society (EMBC), 2020, pp. 3779–3782. doi:10.1109/  
 815 EMBC44109.2020.9176213.
- 816 [32] T. Oku, S. Furuya, A novel vibrotactile biofeedback device for optimiz-  
 817 ing neuromuscular control in piano playing, in: 2019 IEEE Conference  
 818 on Virtual Reality and 3D User Interfaces (VR), 2019, pp. 1554–1555.  
 819 doi:10.1109/VR.2019.8797765.
- 820 [33] Q. Zhu, X.l. Kong, Y.y. Xie, The influence of biofeedback on respiratory  
 821 training effect, in: 2012 International Conference on Systems and Infor-  
 822 matics (ICSAI2012), 2012, pp. 1067–1071. doi:10.1109/ICSAI.2012.  
 823 6223218.
- 824 [34] W. Sangngoen, W. Sroykham, S. Khemthong, W. Jalayondeja, Y. Kajorn-  
 825 predanon, S. Thanangkul, Effect of emg biofeedback on muscle activity in  
 826 computer work, in: The 5th 2012 Biomedical Engineering International  
 827 Conference, 2012, pp. 1–4. doi:10.1109/BMEiCon.2012.6465453.
- 828 [35] An application of bio-feedback in the rehabilitation of the blind, Applied  
 829 Ergonomics 11 (1980) 31–33.
- 830 [36] B.M. Maars Singh, J. Bos, C.F. Van Tuijn, S.B. Renard, Changing stress  
 831 mindset through stressjam: A virtual reality game using biofeedback,  
 832 Games for Health Journal 8 (2019) 326–331.
- 833 [37] M. van Rooij, A. Lobel, O. Harris, N. Smit, I. Granic, Deep: A biofeed-  
 834 back virtual reality game for children at-risk for anxiety, in: Proceedings  
 835 of the 2016 CHI Conference Extended Abstracts on Human Factors in  
 836 Computing Systems, CHI EA '16, Association for Computing Machinery,  
 837 New York, NY, USA, 2016, p. 1989–1997. URL: <https://doi.org/10.1145/2851581.2892452>. doi:10.1145/2851581.2892452.
- 838 [38] R. Blendowske, Unaided visual acuity and blur: a simple model, Optom-  
 839 etry and Vision Science 92 (2015) e121–e125.
- 840 [39] B. Bhattacharyya, D. Bhattacharya, Textbook of Visual Science and Clin-  
 841 ical Optometry, Jaypee Bros. Medical Publishers., 2009.
- 842 [40] W.J. Benjamin, Borish's Clinical Refraction-E-Book, Elsevier Health Sci-  
 843 ences, 2006.
- 844 [41] A. Fajardo Jaimes, F. Rangel de Sousa, Simple modeling of photovoltaic  
 845 solar cells for indoor harvesting applications, Solar Energy 157 (2017)  
 846 792–802.
- 847 [42] Datasheet z03 emg preamplifier, [https://www.motion-labs.com/prod\\_preamp.html#Z03](https://www.motion-labs.com/prod_preamp.html#Z03), ????. (Accessed on 05/21/2023).
- 848 [43] Datasheet ina128, <https://www.ti.com/product/es-mx/INA128>,  
 849 ????. (Accessed on 05/21/2023).
- 850 [44] Datasheet opa2132, <https://www.ti.com/lit/ds/symlink/opa2132.pdf>, ????. (Accessed on 05/21/2023).
- 851 [45] D. Stegeman, H. Hermens, Standards for surface electromyography: The  
 852 european project surface emg for non-invasive assessment of muscles (se-  
 853 niam). 2007, View Article (2007).
- 854 [46] C.J. De Luca, L.D. Gilmore, M. Kuznetsov, S.H. Roy, Filtering the sur-  
 855 face emg signal: Movement artifact and baseline noise contamination,  
 856 Journal of biomechanics 43 (2010) 1573–1579.
- 857 [47] D. Roman-Liu, M. Konarska, Characteristics of power spectrum density  
 858 function of emg during muscle contraction below 30% mvc, Journal of  
 859 Electromyography and Kinesiology 19 (2009) 864–874.
- 860 [48] Datasheet usb-6366, <https://www.ni.com/docs/en-US/bundle/pxie-usb-6366-specs/page/specs.html>, ????. (Accessed on  
 861 05/21/2023).
- 862 [49] Datasheet amc1200, <https://www.ti.com/lit/ds/symlink/amc1200.pdf?ts=1686081409697>, ????. (Accessed on 05/21/2023).
- 863 [50] Datasheet pga281, <https://www.ti.com/lit/ds/symlink/pga281.pdf?ts=1686032914310>, ????. (Accessed on 05/21/2023).

870 **Declaration of generative AI and AI-assisted technologies in  
 871 the writing process**

872 During the preparation of this work the author(s) used [Quill-  
 873 bot, Grammarly and ChatGPT] in order to [enhance its orthog-  
 874 raphy, grammatical style, fluency, coherency, and conciseness].  
 875 After using this tool/service, the author(s) reviewed and edited  
 876 the content as needed and take(s) full responsibility for the con-  
 877 tent of the publication.

## Highlights

- The presbyopia can be corrected using electrically tunable lenses.
- Tunable lenses could be controlled by the human being using biofeedback system.
- A biofeedback system that involves human's senses and brain is difficult to model.
- The biofeedback system controllability is a hard task, which is developed by surveys.
- Smart clinical test could be made to assess the biofeedback system controllability.
- The developed experimental setup shows the human controllability of tunable lenses.

**Declaration of interests**

The authors declare that they have no known competing financial interests or personal relationships that could have appeared to influence the work reported in this paper.

**Conflict of Interest and Authorship Conformation Form**

All authors have participated in (a) conception and design, or analysis and interpretation of the data; (b) drafting the article or revising it critically for important intellectual content; and (c) approval of the final version.

This manuscript has not been submitted to, nor is under review at, another journal or other publishing venue.

The authors have no affiliation with any organization with a direct or indirect financial interest in the subject matter discussed in the manuscript